

Measurement of the magnetization of thin-film samples subjected to mechanical stress

Michael Löffler¹, Ruben Piepgras¹, Alexander Sutor¹, Reinhard Lerch¹

¹Chair of Sensor Technology, Friedrich-Alexander-University Erlangen-Nuremberg, Germany,
 michael.loeffler@fau.de

Abstract – This contribution proposes a method to measure the magnetization of ferromagnetic thin-film samples subjected to mechanical stress. We present our Vector Vibrating Sample Magnetometer and two fixtures that enable the adjustable bending of the ferromagnetic samples during the magnetization measurement. The bending, in turn, results in internal stresses. According to the magnetoelastic effect, the magnetization of ferromagnetic materials depends on internal mechanical stress. Results of two Fe₄₉Co₄₉V₂ samples are shown which prove the applicability of the proposed method.

I. INTRODUCTION

The magnetization of ferromagnetic materials showing magnetostrictive behavior is significantly altered when subjected to mechanical stress. The so-called Villari effect is used in various sensors to measure physical quantities, e.g. torque, stress and force [1, 2].

In order to predict the hysteretic behavior of such materials, we proposed a Preisach-based vector model to enable the simulation of rotational magnetization vectors [3]. The free parameters of the model are identified applying an inverse method to minimize the deviation between simulated and measured data. Thus, measurements of the magnetization of a specific material have to be carried out prior to the simulation of the hysteretic behavior. This is usually done by means of a Vector Vibrating Sample Magnetometer (VVSM).

It has already been shown that our Preisach-based approach is suitable to model ferroelectric hysteretic behavior incorporating mechanical stress [4]. However, the applicability for the stress-dependent magnetization of magnetostrictive materials yet has to be shown.

In this paper, we present our modified VVSM which can be used to measure the magnetization of mechanically prestressed magnetic thin films. KTENA et al. recently published VSM results of electrical steel laminates which were subjected to tensile stress using an INSTRON machine [5]. However, they focused on inelastic strain of the samples. LINVILLE et al. proposed a fixture with a constant radius in order to bend and therefore stress the ferromagnetic samples [6]. We utilize a fixture which allows for the adjustment of the resulting bending instead of a single, fixed

bending/stress.

The paper is organized as follows: In section II, a brief view on the operating principle of our VVSM is given. Afterwards, the fixtures to apply mechanical stress to the samples are presented. In section IV, measurement results of two Fe₄₉Co₄₉V₂ samples are discussed. This paper summarizes the work and concludes with Section V.

II. OPERATING PRINCIPLE OF A VECTOR VIBRATING SAMPLE MAGNETOMETER

The first Vibrating Sample Magnetometer (VSM) was described by FONER in 1959 [7]. The theory and operating principle of a VSM is extensively treated in literature [8] and is therefore only briefly explained here.

In order to magnetize a ferromagnetic sample, it is placed into the air gap of a ferrite yoke with an attached coil. The total magnetic flux density through nearby pickup coils, \vec{B}_{tot} , is composed of the homogenous magnetic field caused by the electromagnet, \vec{B}_{ext} , and the flux density caused by the magnetized sample, \vec{B}_{sample} :

$$\vec{B}_{\text{tot}} = \vec{B}_{\text{ext}} + \vec{B}_{\text{sample}}. \quad (1)$$

Due to the vibration of the ferromagnetic sample, \vec{B}_{sample} varies sinusoidally and therefore a voltage

$$\begin{aligned} u_{\text{ind}}(t) &= - \iint_A \frac{\partial \vec{B}_{\text{tot}}}{\partial t} \cdot d\vec{A} + \underbrace{\oint_C (\vec{v} \times \vec{B}_{\text{tot}}) \cdot d\vec{s}}_{=0} \\ &= - \iint_A \left(\underbrace{\frac{\partial \vec{B}_{\text{ext}}}{\partial t}}_{=0} + \frac{\partial \vec{B}_{\text{sample}}}{\partial t} \right) \cdot d\vec{A} \end{aligned} \quad (2)$$

is induced in the pickup coils. Note that the term $\vec{v} \times \vec{B}_{\text{tot}}$ becomes zero because the pickup coils are mounted stationary. Since \vec{B}_{ext} is constant in respect of time and position and B_{sample} is proportional to the magnetization M , after calibration of the whole setup the magnetization of any kind of material sample can be measured by metering the induced voltage at a specific applied magnetic field.

The out-of-plane component of the magnetization vector of very thin ferromagnetic films with a thickness of only a few micrometers is negligible, thus \vec{M} can be resolved

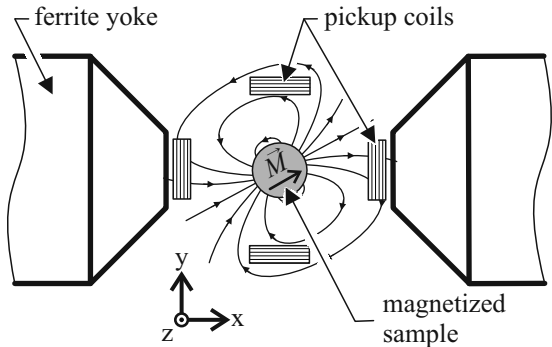


Fig. 1. Schematic of the Vector Vibrating Sample Magnetometer. For reasons of clarity, only the magnetic flux density \vec{B}_{sample} resulting from the magnetization \vec{M} of the sample is shown. The flux density \vec{B}_{ext} caused by the electromagnet is not indicated instead.

into a component \vec{M}_{\parallel} parallel (in x -direction, cf. Figure 1) and a component \vec{M}_{\perp} perpendicular (in y -direction) to the external magnetic field,

$$\vec{M} = \vec{M}_{\perp} + \vec{M}_{\parallel}. \quad (3)$$

With a view to measuring the two components of the magnetization vector simultaneously the VSM is extended by a second pair of pickup coils oriented perpendicularly to the first pair of coils [9]. The whole setup is depicted schematically in Figure 1. The induced voltages are proportional to the particular magnetization components,

$$\hat{u}_{\text{ind},\perp} \propto M_{\perp} \quad \text{and} \quad \hat{u}_{\text{ind},\parallel} \propto M_{\parallel}, \quad (4)$$

respectively. Prior to carrying out measurements, the VSM has to be calibrated. This is usually done with the help of a sample of known dimensions and saturation polarization (e.g. Mu-metal).

Besides the ability to determine the single magnetization components, the advantage of our Vector Vibrating Sample Magnetometer (VVSM) is that the samples can be rotated during measurement. Hence, the rotation of the magnetization vector of anisotropic thin films can be evaluated.

III. MECHANICAL PRESTRESSING OF FERROMAGNETIC SAMPLES

The magnetoelastic effect states that a change of the mechanical stress applied to a magnetic probe entails a change in its magnetization. It was our goal to alter the VVSM in such a way that the effect of magnetoelasticity on the probe's magnetization could be measured. In order to do so, a fixture to apply stress on the probe and maintain it during the whole duration of the measurement had to be designed.

The nature of the measurement setup imposes restrictions concerning the size, weight and material of the sample fixture. The size restrictions are due to the small size of the air gap between the sections of the electromagnet. Axial symmetry is crucial in order to avoid lateral vibrations. Limitations to the weight are determined by the shaker which ensures the sinusoidal vibration of the sample. Finally, the materials used in proximity of the ferromagnetic sample have to be dia- or paramagnetic to not influence the measurement. Thus, acrylic glass and brass were used to manufacture the fixtures for the sample.

We chose an indirect approach similar to the method presented in [6] to bend the samples and therefore generate mechanical stress inside. In a first step, we used a fixture as depicted schematically in Figure 2.

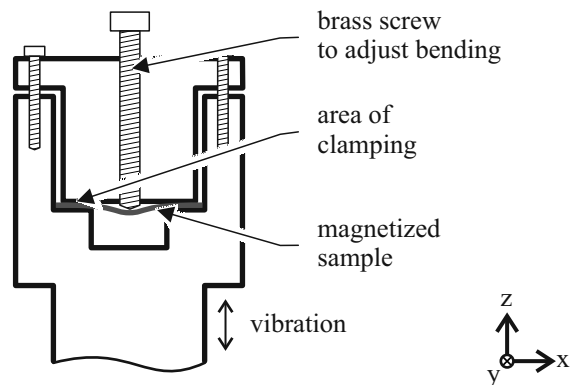


Fig. 2. Cross section of the fixture to obtain an adjustable bending of the ferromagnetic sample. A screw is used to generate a normal force on the thin film. The screw is attached to a transmission device (not shown) to precisely adjust the deflection. Due to the clamping at the edge of the sample, tensile and compressive stresses occur inside the material.

The basic idea behind it is that by applying a normal force on the middle of the thin layer a bending moment is created which induces a change of internal stress within the material. This force is generated via a brass screw with a small pitch. The screw can be attached to a transmission device, therefore the deflection w at the center of the material can be adjusted precisely (maximum error $\pm 10 \mu\text{m}$). Furthermore, the screw and the material are used as electrical electrodes. Hence, the point of first contact can be determined by measuring the electrical resistance between the two electrodes.

Due to the clamping at the edge of the sample, tensile and compressive stress components occur. Although tensile and compressive stress have opposite effects on the magnetization of the sample, we expect a measurable change in the net magnetization according to results presented in [10], where a magnetoelastic pressure sensor was

proposed.

In order to apply a well-defined bending stress on the material sample during measurement, a second fixture was manufactured. The cross section of this fixture is shown schematically in Figure 3. The bottom part of the sample

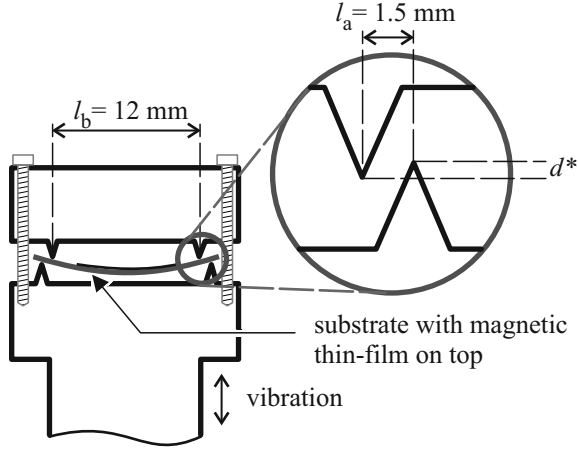


Fig. 3. Cross section of the second fixture to apply a known bending stress on sputter-deposited material samples. The stress inside the thin film can be derived precisely by measuring the displacement $d = d^* + h_{\text{substrate}}$.

holder is fixated on the vibrating rod. The upper part can be moved downwards via two fine-thread brass screws. The distance between the two segments respectively the displacement d (cf. Figure 3) is determined using a precise micrometer screw gauge. Thus, the maximum displacement error is $\Delta d = \pm 5 \mu\text{m}$.

By means of this sample holder, the stress σ_{sample} inside a sputter-deposited magnetic thin film with a height h_{sample} much smaller than the height $h_{\text{substrate}}$ of the used substrate yields

$$\sigma_{\text{sample}} = E_{\text{sample}} \cdot \varepsilon_{\text{sample}} = E_{\text{sample}} \cdot \frac{h_{\text{substrate}}}{2 \cdot \rho}, \quad (5)$$

where E_{sample} denotes the Young's modulus of the magnetic thin film, $\varepsilon_{\text{sample}}$ the strain of the sample and ρ the neutral bending radius of the substrate.

Assuming pure bending (neither normal nor shear forces inside the substrate), the neutral bending radius can be determined by evaluating

$$\rho = \frac{l_b}{2 \cos\left(\frac{\pi}{2} - \arctan\left(\frac{d}{l_a}\right)\right)}, \quad (6)$$

with the dimensions d , l_a and l_b illustrated in Figure 3. Thus, by using this fixture, resulting stress inside the magnetic thin film can be calculated by determining the displacement d of the upper part of the sample holder. By

flipping over the substrate, compressive as well as tensile stress can be applied.

IV. RESULTS

In Figure 4, measured hysteresis loops of a $\text{Fe}_{49}\text{Co}_{49}\text{V}_2$ sample ($\varnothing = 10 \text{ mm}$, $h_{\text{sample}} = 42 \mu\text{m}$) using the fixture with clamped material edges (cf. Figure 2) are shown.

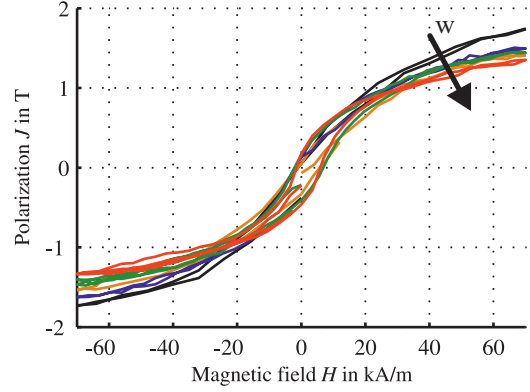


Fig. 4. Polarization hysteresis of $\text{Fe}_{49}\text{Co}_{49}\text{V}_2$ for different central deflections w of the sample. As a reference, the measurement results of the unstressed sample are depicted (black line). The deflection was increased stepwise up to 0.5 mm with a maximum error of $\pm 10 \mu\text{m}$.

In order to analyze the effect of bending on the sample's magnetization the hysteresis loops under various central deflections w were evaluated. To get a reference loop, the first measurement was done using the unstressed sample. Afterwards, the central deflection and therefore the bending was increased stepwise up to $w = 0.5 \text{ mm}$. As can be seen from the obtained results, the polarization of the sample varies with the applied bending.

In Figure 5, the remanent and saturation polarization of the sample are depicted as a function of the central deflection. Whereas the saturation polarization declines significantly (up to -25%) with the applied deflection, the remanent polarization increases (up to 350%). We relate both effects to the internal compressive and tensile stress and accompanying impairment respectively support of magnetic domain movement and rotation.

The deflection-dependent coercive field strength is shown in Figure 6. Due to the very small (ideally zero at coercive field strength) induced voltages at this magnetization state the signals are more prone to noise and the resulting error is rather high. Therefore, no clear dependence can be deduced.

A second thin film sample was prepared by sputter-depositing $\text{Fe}_{49}\text{Co}_{49}\text{V}_2$ on a sheet of brass. The dimensions and parameters of the resulting sample are listed in

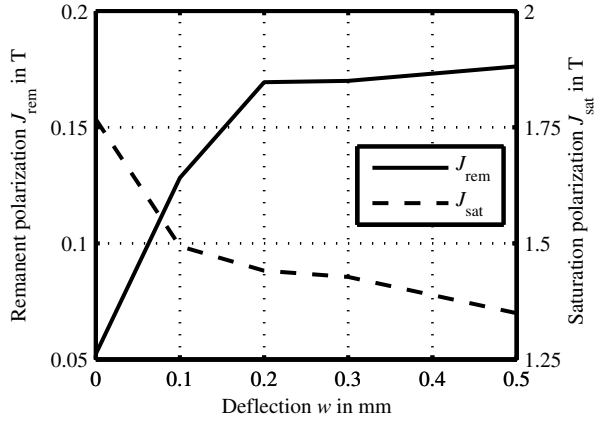


Fig. 5. Remanent polarization J_{rem} and saturation polarization J_{sat} of the clamped $\text{Fe}_{49}\text{Co}_{49}\text{V}_2$ sample as a function of central deflection w .

Table 1. Dimensions and Young's modulus of the thin film sample. The height of the magnetic film was measured with the help of a confocal microscope.

$h_{\text{substrate}}$	200 μm
h_{sample}	3 μm
$\varnothing_{\text{sample}}$	10 mm
E_{sample}	230 GPa

Table 1.

By means of the second fixture (cf. Figure 3), the thin film was stressed and hysteresis measurement were carried out. In Figure 7, the measured hysteresis curves as a function of the applied compressive stress / strain are depicted. Compared to the results of the bulk sample presented in Figure 4, the saturation polarization of the sputtered, unstressed $\text{Fe}_{49}\text{Co}_{49}\text{V}_2$ is slightly lower. As can be seen in Figure 8, due to the almost uniform compressive stress both the saturation (up to -37%) and remanent polarization (up to -58%) of the thin film decrease with the applied compressive stress. Again, a clear correlation between coercive field strength and stress can not be inferred, cf. Figure 9.

V. CONCLUSION

In this paper, we presented a method to measure the stress-dependent magnetization of ferromagnetic thin films by means of a Vibrating Sample Magnetometer. The stress inside the sample is applied via fixtures that allow the adjustment of the bending of the sample. The presented results show that the hysteresis of $\text{Fe}_{49}\text{Co}_{49}\text{V}_2$ is significantly altered when subjected to stress. Saturation and remanent polarization of the material strongly depend on the

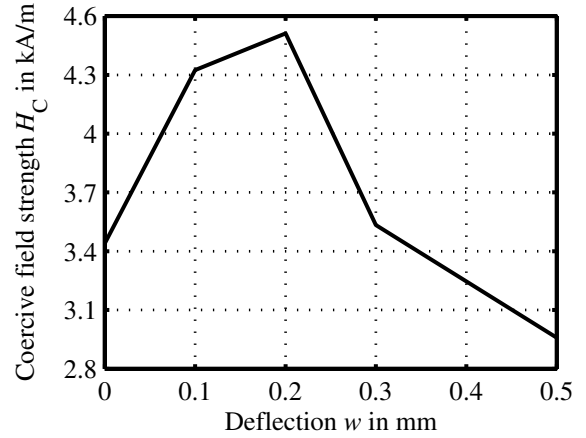


Fig. 6. Coercive field strength H_C of the clamped $\text{Fe}_{49}\text{Co}_{49}\text{V}_2$ sample as a function of central deflection w .

applied stress.

As a next step, we will investigate the suitability of our Preisach based vector model for stressed ferromagnetic samples. Furthermore, other magnetoelastic materials such as Metglas will be investigated to deduce their applicability for sensors based on the magnetostrictive/magnetoelastic effect.

VI. REFERENCES

- [1] N. Ekreem, A. Olabi, T. Prescott, A. Rafferty, and M. Hashmi, "An overview of magnetostriction, its use and methods to measure these properties," *Journal of Materials Processing Technology*, vol. 191, pp. 96–101, Aug. 2007.
- [2] T. Huber, B. Bergmair, C. Vogler, F. Bruckner, G. Hrkac, and D. Suess, "Magnetoelastic resonance sensor for remote strain measurements," *Applied Physics Letters*, vol. 101, no. 4, p. 042402, 2012.
- [3] A. Sutor, J. Kallwies, and R. Lerch, "An efficient vector Preisach hysteresis model based on a novel rotational operator," *Journal of Applied Physics*, vol. 111, no. 7, p. 07D106, 2012.
- [4] F. Wolf, A. Sutor, S. J. Rupitsch, and R. Lerch, "A generalized Preisach approach for piezoceramic materials incorporating uniaxial compressive stress," *Sensors and Actuators A: Physical*, vol. 186, pp. 223–229, Oct. 2012.
- [5] A. Ktena, D. Davino, C. Visone, and E. Hristoforou, "Stress dependent vector magnetic properties in electrical steel," *Physica B: Condensed Matter*, vol. 435, pp. 25–27, Feb. 2014.
- [6] E. Linville, D. Han, J. Judy, and J. Sivertson, "Stress effects on the magnetic properties of FeMn and NiMn spin valves," *IEEE Transactions on Magnetics*, vol. 34, no. 4, pp. 894–896, 1998.

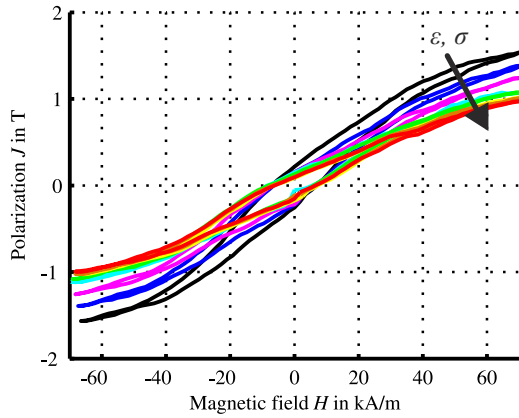


Fig. 7. Polarization hysteresis of sputter-deposited $Fe_{49}Co_{49}V_2$ on a brass substrate for different strain ϵ respectively stress σ . As a reference, the measurement results of the unstressed sample are depicted (black line). The strain was increased stepwise up to 0.83 %.

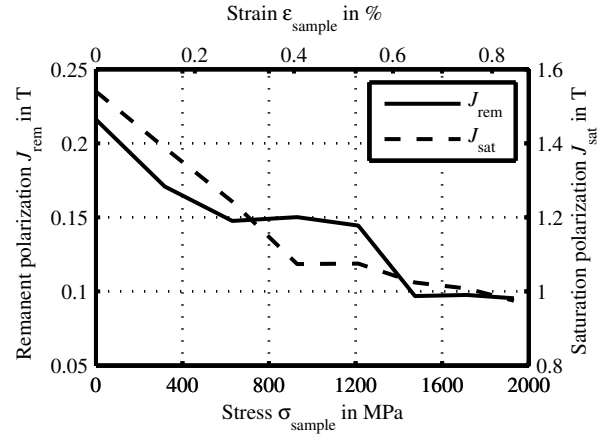


Fig. 8. Remanent polarization J_{rem} and saturation polarization J_{sat} of the sputter-deposited $Fe_{49}Co_{49}V_2$ as a function of strain ϵ_{sample} respectively stress σ_{sample} .

- [7] S. Foner, "Versatile and Sensitive Vibrating-Sample Magnetometer," *Review of Scientific Instruments*, vol. 30, no. 7, pp. 548–557, 1959.
- [8] A. Pacyna and K. Ruebenbauer, "General theory of a vibrating magnetometer with extended coils," *Journal of Physics E: Scientific Instruments*, vol. 141, 1984.
- [9] L. Benito, J. I. Arnaudas, and A. del Moral, "High-sensitivity vector magnetometer for measuring magnetic torque at low temperatures," *Review of Scientific Instruments*, vol. 77, no. 2, p. 025101, 2006.
- [10] H.-C. Chang, S.-C. Liao, H.-S. Hsieh, S.-J. Lin, C.-H. Lai, R. Chen, and W. Fang, "A novel inverse-magnetostrictive type pressure sensor with planar sensing inductor," *2013 IEEE 26th International Conference on Micro Electro Mechanical Systems (MEMS)*, pp. 685–688, Jan. 2013.

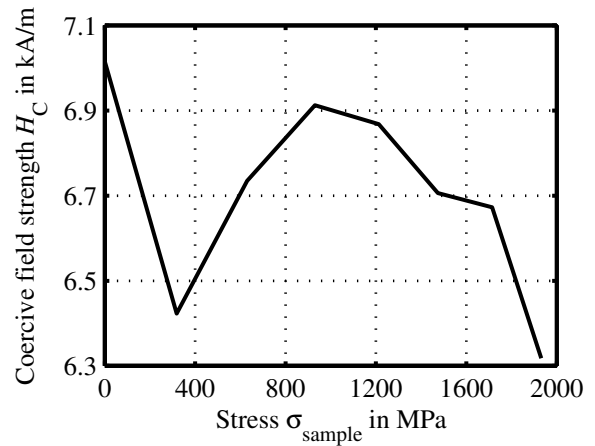


Fig. 9. Coercive field strength H_C of the thin film $Fe_{49}Co_{49}V_2$ as a function of stress σ_{sample} .